

---

---

# Dose Response of Pancreatic Neuroendocrine Tumors Treated with Peptide Receptor Radionuclide Therapy Using $^{177}\text{Lu}$ -DOTATATE

Ezgi Ilan<sup>1,2</sup>, Mattias Sandström<sup>1,2</sup>, Cecilia Wassberg<sup>1,3</sup>, Anders Sundin<sup>1,3</sup>, Ulrike Garske-Román<sup>1,3</sup>, Barbro Eriksson<sup>4</sup>, Dan Granberg<sup>4</sup>, and Mark Lubberink<sup>1,2</sup>

<sup>1</sup>Nuclear Medicine and PET, Department of Radiology, Oncology, and Radiation Science, Uppsala University, Uppsala, Sweden; <sup>2</sup>Medical Physics, Uppsala University Hospital, Uppsala, Sweden; <sup>3</sup>Molecular Imaging, Medical Imaging Centre, Uppsala University Hospital, Uppsala, Sweden; and <sup>4</sup>Section of Endocrine Oncology, Department of Medical Science, Uppsala University Hospital, Uppsala, Sweden

Peptide receptor radionuclide therapy (PRRT) is a promising treatment for patients with neuroendocrine tumors, giving rise to improved survival. Dosimetric calculations in relation to PRRT have been concentrated to normal organ dosimetry in order to limit side effects. However, the relation between the absorbed dose to the tumor and treatment response has so far not been established. Better knowledge in this respect may improve the understanding of treatment effects, allow for improved selection of those patients who are expected to benefit from PRRT, and avoid unnecessary treatments. The aim of the present work was to evaluate the dose–response relationship for pancreatic neuroendocrine tumors treated with PRRT using  $^{177}\text{Lu}$ -DOTATATE. **Methods:** Tumor-absorbed dose calculations were performed for 24 lesions in 24 patients with metastasized pancreatic neuroendocrine tumors treated with repeated cycles of  $^{177}\text{Lu}$ -DOTATATE at 8-wk intervals. The absorbed dose calculations relied on sequential SPECT/CT imaging at 24, 96, and 168 h after infusion of  $^{177}\text{Lu}$ -DOTATATE. The unit density sphere model from OLINDA was used for absorbed dose calculations. The absorbed doses were corrected for partial-volume effect based on phantom measurements. On the basis of these results, only tumors larger than 2.2 cm in diameter at any time during the treatment were included for analysis. To further decrease the effect of partial-volume effect, a subgroup of tumors (>4.0 cm) was analyzed separately. Tumor response was evaluated by CT using Response Evaluation Criteria In Solid Tumors. **Results:** Tumor-absorbed doses until best response ranged approximately from 10 to 340 Gy. A 2-parameter sigmoid fit was fitted to the data, and a significant correlation between the absorbed dose and tumor reduction was found, with a Pearson correlation coefficient ( $R^2$ ) of 0.64 for tumors larger than 2.2 cm and 0.91 for the subgroup of tumors larger than 4.0 cm. The largest tumor reduction was 57% after a total absorbed dose of 170 Gy. **Conclusion:** The results imply a significant correlation between absorbed dose and tumor reduction. However, further studies are necessary to address the large variations in response for similar absorbed doses.

**Key Words:**  $^{177}\text{Lu}$ -DOTATATE; dose-response; neuroendocrine tumors; dosimetry; RECIST

**J Nucl Med 2015; 56:177–182**

DOI: 10.2967/jnumed.114.148437

**D**uring the last decade, peptide receptor radionuclide therapy (PRRT) with radiolabeled somatostatin analogs such as  $^{177}\text{Lu}$ -DOTATATE and  $^{90}\text{Y}$ -DOTATOC has shown to be an effective treatment in patients with neuroendocrine tumors (NETs). This treatment method plays an increasingly important role in the treatment of NETs (1–9), particularly of disseminated pancreatic NETs (PNETs) (3). PNETs are tumors that vary in clinical aggressiveness depending on the subtype (functional or nonfunctional) and histologic features (Ki-67 index, mitotic count). These tumors have a relatively poor prognosis among NETs in terms of survival rate. For patients with metastatic PNETs, the 5-y survival rate was 27% (10). According to U.S. Surveillance, Epidemiology, and End Results program registries, the overall annual incidence of PNETs was 0.32 per 100,000 individuals.

Erasmus University Hospital in Rotterdam, The Netherlands, which has the most extensive experience in PRRT with  $^{177}\text{Lu}$ -DOTATATE for NETs, reported their results in more than 500 NET patients, showing complete or partial remission in 30% and minor response in 16% of the patients (3). Median progression-free survival was 40 mo, and median overall survival was 46 mo from the start of treatments and 128 mo from diagnosis. These results were considered an improvement as compared with historic controls. Since 2005, more than 400 patients have undergone PRRT with  $^{177}\text{Lu}$ -DOTATATE at Uppsala University Hospital, showing similar results (11). Since 2009, all treated patients are enrolled in a dosimetry-based prospective study; these patients are selected on the basis of the tumor uptake of  $^{111}\text{In}$ -DTPA-D-Phe<sup>1</sup>-octreotide (OctreoScan; Mallinckrodt, Inc.) on their planar scintigraphy images. Patients with tumor uptake of grades 3 or 4 according to the Krenning scale (higher uptake than the normal liver) (2,5) are considered suitable for PRRT. The standard administered activity (intravenously) is 7.4 GBq of  $^{177}\text{Lu}$ -DOTATATE per cycle, with a 6- to 8-wk interval between cycles (12,13).

Theoretically, in PRRT, the best result is obtained when the absorbed dose to normal organs is close to the maximum-tolerated dose for the organs at risk. The number of administered treatment cycles is therefore restricted by the maximum acceptable absorbed doses to the kidneys and bone marrow, which are the dose-limiting organs (12–16). In the protocol used at Uppsala, the maximum accepted doses were set to 23 Gy to the kidneys and 2 Gy to the bone marrow. Better knowledge of the absorbed doses to the tumor may allow for improved selection of those patients who are expected to benefit from PRRT and avoid unnecessary treatments to those who will not.

---

Received Sep. 12, 2014; revision accepted Dec. 15, 2014.  
For correspondence or reprints contact: Ezgi Ilan, Uppsala University Hospital, Section of Medical Physics, SE-751 85 Uppsala, Sweden.  
E-mail: ezgi.ilan@akademiska.se  
Published online Jan. 15, 2015.  
COPYRIGHT © 2015 by the Society of Nuclear Medicine and Molecular Imaging, Inc.

In addition to the sparse temporal sampling of imaging data that affects accuracy of absorbed dose estimates for large organs (13), quantitative estimates of tumor activity concentrations with SPECT are also hampered by the spatial resolution of SPECT, resulting in large partial-volume effects (PVEs).

Large intrapatient and intralesion variability in tumor uptake has been observed in PRRT of NETs (17). Interestingly, to our knowledge, only 1 study has reported on the tumor-absorbed dose–response relationship in connection with PRRT using <sup>90</sup>Y-DOTATOC (18). This study showed a significant correlation ( $R^2 = 0.50$ ) between tumor reduction and absorbed dose, as estimated using the MIRDOSE (MIRD) sphere model and based on <sup>86</sup>Y-DOTATOC PET measurements. However, no dose–response relationship has yet been reported for NETs using <sup>177</sup>Lu-DOTATATE. The aim of the present study was to estimate the absorbed doses to PNETs and to investigate the tumor-absorbed dose–response relationship for PNETs treated with <sup>177</sup>Lu-DOTATATE.

## MATERIALS AND METHODS

### Patients and Therapy

The patients were selected among those enrolled in a prospective study (EudraCT nr 2009-012660-14) approved by the Regional Ethical Review board and the board for Radiation Ethics in Uppsala. The patients were

included after giving their written informed consent. Briefly, the patients had metastasized NETs with intense somatostatin receptor expression, as confirmed by somatostatin receptor scintigraphy with <sup>111</sup>In-DTPA-D-Phe<sup>1</sup>-octreotide. They had undergone a full treatment with <sup>177</sup>Lu-DOTATATE, that is, until they had received an accumulated absorbed dose of 23 Gy to the kidneys or 2 Gy to the bone marrow. In the present study, patients with PNETs were selected with the presence of 1 tumor with a diameter larger than 2.2 cm at any time during the treatment, as explained later. Of 40 treated patients with PNETs, 24 patients (11 women and 13 men; age, 43–78 y) had tumors larger than 2.2 cm.

DOTATATE was obtained as a generous gift from Prof. Eric Krenning (Erasmus Medical Center), and <sup>177</sup>LuCl<sub>3</sub> was purchased from IDB. Labeling of DOTATATE was performed in-house at Uppsala University Hospital. <sup>177</sup>Lu-DOTATATE was diluted in 100 mL of saline and infused intravenously during 30 min, followed by 15-min rinsing with physiologic saline. For kidney protection, all patients received 2 L of commercially available mixed amino acid solution (Vamin, 14 gN/L, without added electrolytes; Fresenius Kabi) infused during 8 h, starting 30 min before treatment, at a rate of 250 mL/h (12,13).

Patients were treated with 2–6 cycles of <sup>177</sup>Lu-DOTATATE. The individual number of cycles was determined by the maximum estimated absorbed doses to the kidneys and bone marrow, which were set to 23 and 2 Gy, respectively. The dosimetry approach has been described in detail elsewhere (12,13). The time interval between each treatment cycle was 6–8 wk. In Table 1,

**TABLE 1**  
Details of Patient Cohort Treated with <sup>177</sup>Lu-DOTATATE

Patient no.	Sex	No. of tumors	A <sub>1</sub> (GBq)	A <sub>2</sub> (GBq)	A <sub>3</sub> (GBq)	A <sub>4</sub> (GBq)	A <sub>5</sub> (GBq)	A <sub>6</sub> (GBq)
1	Female	2	7.4*	7.4	7.4	7.4*	7.4	7.4
2	Female	1	7.4*	7.4	7.4	7.4	—	—
3	Female	1	7.4*	7.4	7.4	7.4*	7.4	—
4	Male	3	7.4*	7.4	6.0	—	—	—
5	Male	1	7.4*	7.4	7.4	—	—	—
6	Male	1	7.4*	7.4	7.4	7.4*	—	—
7	Female	1	7.4*	7.4	7.4	7.4*	7.4	—
8	Female	1	7.4*	7.4	7.4	7.4*	7.4	7.4
9	Male	2	7.4*	7.4	7.4*	7.4	7.4	—
10	Male	1	7.4*	7.4	7.4	7.4*	—	—
11	Male	3	7.4*	7.4	—	—	—	—
12	Male	1	7.4*	7.4	6.0*	7.4	7.4*	—
13	Male	2	7.4*	7.4*	7.4	7.4	—	—
14	Female	2	7.4*	7.4	6.0*	7.4	—	—
15	Female	1	7.4*	5.0	7.4*	4.0	—	—
16	Male	1	7.4*	7.4	7.4	7.4*	—	—
17	Male	4	7.4*	7.4	7.4*	7.4	—	—
18	Male	1	7.4*	7.4	7.4*	7.4	—	—
19	Female	1	7.4*	7.4	7.4*	—	—	—
20	Female	3	7.4*	7.4	7.4*	7.4	7.4	—
21	Male	1	7.4*	7.4	7.4*	—	—	—
22	Female	4	7.4*	7.4	7.4	7.4*	—	—
23	Female	1	7.4*	7.4	5.0*	—	—	—
24	Male	3	7.4*	5.0	5.0*	—	—	—

\*Complete dosimetric evaluation.

A<sub>1–6</sub> is amount of administered activity at each treatment up to 6 cycles.

a summary of the patient cohort with sex, number of tumors, and administered activity at each cycle (A1–A6) is presented.

### Image Acquisition and Reconstruction

At the first and one of the later (third or fifth) therapy cycles, a complete dosimetric evaluation was performed, as described earlier (13,19). This evaluation consisted of SPECT/CT examinations acquired 24, 96, and 168 h after infusion combined with frequent blood sampling to assess bone marrow dosimetry (13,20). During intermediate therapy cycles, patients underwent a single SPECT/CT examination acquired at 24 h after injection.

SPECT/CT of the upper abdomen of patients was performed with a dual-head Infinia Hawkeye SPECT/CT system (GE Healthcare) equipped with 0.952-cm (0.375-in)-thick NaI(Tl) crystals using medium-energy general-purpose collimators. An energy window of 20% was applied around the dominant  $\gamma$ -ray energy (208.4 keV), and SPECT images were acquired with 120 frames at 30 s per frame. Calibration of the SPECT images was performed as described earlier (13). SPECT images were reconstructed using Xeleris (version 2.0; GE Healthcare) with the ordered-subsets expectation maximization algorithm. Default settings were used with 8 subsets and 4 iterations, and a Hanning filter was applied, with a cutoff at 0.85 cycles/cm, including attenuation correction as based on an automatically generated attenuation map created from a 4-slice CT scanner (Hawkeye, 140 keV, 3.0 mA, half rotation).

For response evaluation, CT of the thorax and abdomen was performed using a clinical routine examination protocol whereby the liver was examined before and during intravenous contrast enhancement in the late arterial phase, and the thorax and abdomen were examined in the venous contrast-enhancement phase. CT was performed as a baseline examination before the start of PRRT, before therapy cycles 3 and 5, and 3 mo after therapy. Subsequent follow-up examinations were performed at 6-mo intervals.

### Recovery Coefficients (RCs)

To compensate for underestimation of the activity concentration in the tumor measurements due to PVE, RCs were derived from a phantom measurement (21). RCs were determined by scanning the National Electrical Manufacturers Association image quality phantom (22), containing 6 fillable spheres with diameters ranging from 10 to 37 mm. The measurement was repeated 6 times, with activity concentrations of  $^{177}\text{Lu}$  ranging between 2.7 and 5.5 MBq/mL. There was no background activity in the phantom, and the same reconstruction settings as described above for patient scans were used. Volumes of interest (VOIs) were drawn in all 6 images over each sphere at 42% isocontours, which are expected to most closely resemble actual sphere size (23). RC was defined as the ratio between the measured activity concentration ( $C_M$ ) and actual activity concentration ( $C_A$ ):

$$\text{RC} = \frac{C_M}{C_A} \quad \text{Eq. 1}$$

A 2-parameter sigmoid function (24) was fitted to the mean RC values as a function of sphere diameter:

$$\text{RC}(d) = \frac{100}{1 + \left(\frac{\alpha}{d}\right)^\beta} \quad \text{Eq. 2}$$

where  $d$  is the diameter of the sphere based on the SPECT image, and  $\alpha$  and  $\beta$  are fit parameters. In addition, sphere diameters derived using the 42% isocontour VOIs were compared with the true sphere diameters.

### Dosimetry

The respective largest transversal tumor diameters were measured on the baseline CT examination and on all follow-up CT studies. The absorbed doses were calculated for tumors larger than 2.2 cm in diameter at any time during the treatment, and in addition, to minimize

the PVE on the calculations, a subgroup analysis for tumors larger than 4.0 cm in diameter was performed. Only the largest tumor in each patient was used in the presented analysis.

SPECT/CT examinations were analyzed on a HERMES workstation (Hybrid PRD, version 1.4B; HERMES Medical Solutions AB), and the tumors were delineated by automatic-threshold VOIs using a 42% isocontour. For complete dosimetric evaluations, the activity concentrations were calculated for each scanning time point and corrected for PVEs using Equation 2, assuming a spherical tumor shape. The time-integrated activity concentration was then calculated as the area under the curve of a single exponential fit:

$$\tilde{C} = \int_0^{\infty} C_0 \times e^{-\frac{\ln(2) \times t}{t_{\text{eff}}}} = C_0 \times \frac{t_{\text{eff}}}{\ln(2)} \quad \text{Eq. 3}$$

where  $\tilde{C}$  is the time-integrated activity concentration,  $C_0$  is the activity concentration at time zero, and  $t_{\text{eff}}$  is the effective half-life. For intermediate therapy cycles, during which only a single (24 h after injection) SPECT/CT scan was acquired, the time-integrated activity was computed assuming a similar effective half-life as in the preceding complete dosimetric evaluation, as previously reported for organ dosimetry (19). To verify this assumption of unchanged effective half-life, effective half-lives of subsequent complete dosimetric evaluations were compared in those patients for whom more than 1 complete dosimetric evaluation was performed.

The absorbed dose to the tumors at complete dosimetric evaluation ( $D_C$ ) was calculated using the following equation:

$$D_C = \tilde{C} \times \text{ACDF} \quad \text{Eq. 4}$$

where ACDF is the activity concentration dose factor, calculated as the dose factor (DF) for a 10-g sphere as taken from OLINDA/EXM 1.1 multiplied with the weight of the sphere (12). Only self-dose was considered in the absorbed dose calculations because of the negligible crossfire dose for  $^{177}\text{Lu}$ -DOTATATE. The absorbed dose at limited dosimetry was calculated with the following equation:

$$D_L = D_C \times \frac{C_{24}^L}{C_{24}} \quad \text{Eq. 5}$$

where  $D_C$  is the absorbed dose obtained from previous complete dosimetric evaluation,  $C_{24}$  is the activity concentration at 24 h after

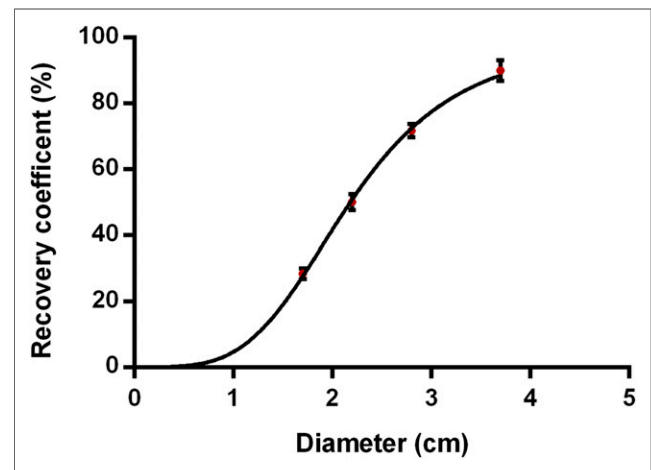


**FIGURE 1.** RC vs. sphere diameter (3.7, 2.8, 2.2, and 1.7). For each sphere in National Electrical Manufacturers Association image quality phantom, 6 RCs were determined, and the mean and SD of these 6 values are shown. Solid line represents 2-parameter sigmoid fit.

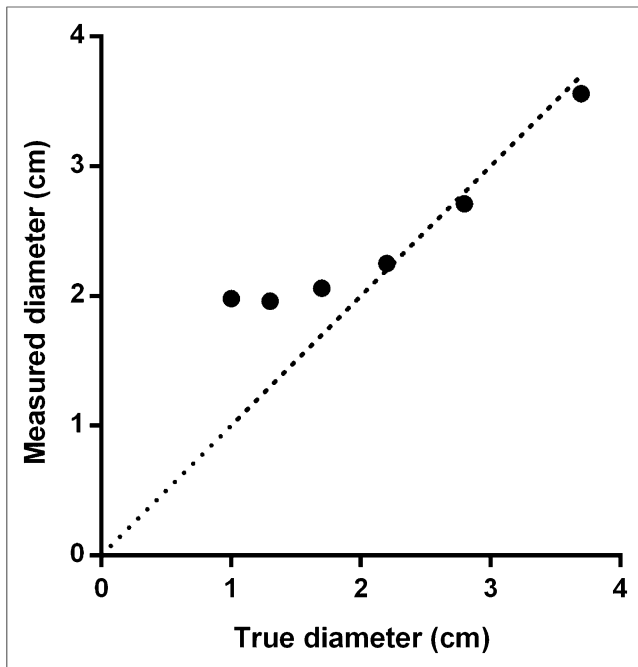


**FIGURE 2.** Measured sphere diameter using a 42% isocontour VOI vs. true sphere diameter in National Electrical Manufacturers Association image quality phantom. Dashed line represents line of identity.

injection from previous complete dosimetric evaluation, and  $C_{24}^L$  is the activity concentration 24 h after injection at limited dosimetry.

#### Best Response Analysis

The overall best response, which is the best response recorded from the start of treatment until disease progression/recurrence, was determined according to Response Evaluation Criteria In Solid Tumors (25). The largest diameter of the tumors was delineated in transaxial diagnostic CT images. The best response was calculated as follows:

$$T_{BR} = \frac{d_B - d_S}{d_B} \times 100, \quad \text{Eq. 6}$$

where  $d_B$  is the diameter of the tumor at baseline, and  $d_S$  is the smallest of the largest diameters of the tumor in the follow-up CT examinations. The absorbed dose until best response was calculated for each tumor by adding the absorbed doses in each therapy cycle until best response.

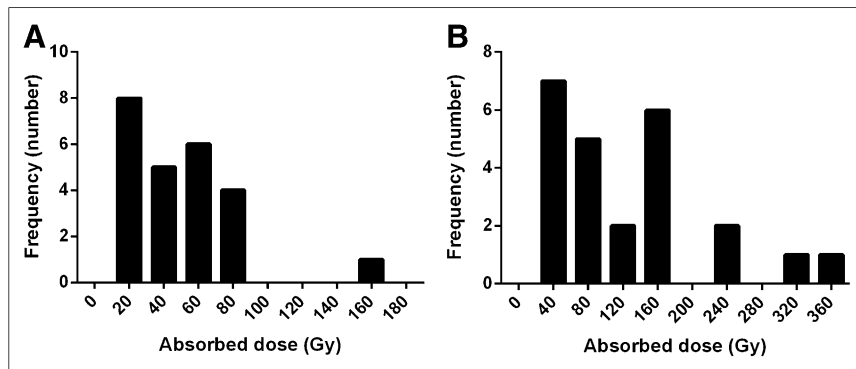


**FIGURE 3.** Frequency distribution of absorbed doses in 24 tumors. (A) Absorbed dose distribution during first treatment cycle. (B) Distribution of tumor-absorbed dose until best response. Numbers on x axes are centers of absorbed dose intervals used for each bar (20 Gy =  $20 \pm 10$  Gy [A], 40 Gy =  $40 \pm 20$  Gy [B]).

## RESULTS

### Recovery Coefficient

The RC as a function of sphere diameter is presented in Figure 1, and Figure 2 illustrates the measured sphere diameter based on 42% isocontour VOIs versus true sphere diameter. The measured diameters were in good agreement with the true diameters for spheres larger than 2.2 cm, whereas there was a severe overestimation for smaller spheres and essentially diameters of spheres smaller than 2.2 cm could not be estimated, rendering partial-volume correction impossible. Hence, tumors with diameter smaller than 2.2 cm were excluded from the study.

### Dosimetry

The frequency distribution of the absorbed dose during the first therapy cycle and the absorbed dose until best response are presented in Figure 3. The most frequent absorbed dose was approximately 20 Gy during the first therapy cycle, with a median of approximately 50 Gy (range, 10–170 Gy) (Fig. 3A), whereas the dose resulting in best response was most frequently reached at approximately 40 Gy (Fig. 3B).

The mean ratio between the effective half-lives during cycles 3 (or 5, where applicable) to 1 was  $0.98 \pm 0.12$ , and the median was 0.98 (range, 0.7–1.3), indicating similar effective half-lives for subsequent treatments.

### Dose–Response Relation

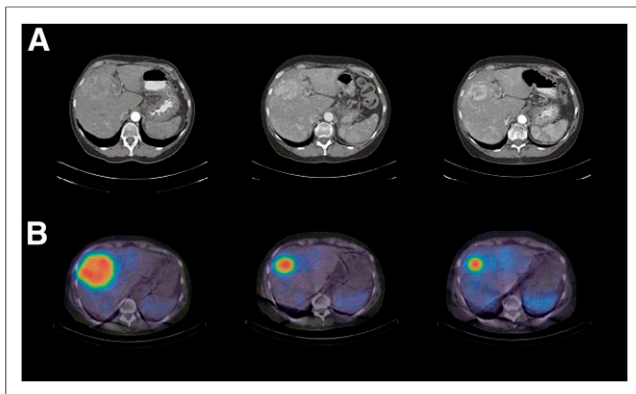
An illustration of tumor response in a patient treated with 3 cycles of  $^{177}\text{Lu}$ -DOTATATE is presented in Figure 4. This patient had a tumor reduction of 29% according to Response Evaluation Criteria In Solid Tumors after a total tumor-absorbed dose of 190 Gy.

Figure 5 presents the relation between the absorbed dose until best response and tumor response, for tumors larger than 2.2 and 4.0 cm, respectively. The tumor response was in the range of 4.5%–57% and the absorbed dose between 20 and 340 Gy for tumors larger than 2.2 cm. The Pearson correlation coefficient ( $R^2$ ) between the absorbed dose and best response for tumors larger than 2.2 cm in diameter was 0.64 and increased significantly to 0.91 for tumors larger than 4.0 cm in diameter. There was, however, no significant difference in the parameters of the sigmoid fits.

## DISCUSSION

Knowledge about the relationship between the tumor-absorbed dose and tumor reduction is crucial for a better understanding of PRRT. The aim of this study was to estimate the absorbed doses to tumors and to investigate the absorbed dose–response relationship for PNETs treated with  $^{177}\text{Lu}$ -DOTATATE. Here, we present the first, to our knowledge, dose–response relation for PNETs treated with PRRT using  $^{177}\text{Lu}$ -DOTATATE.

In a subset of 24 patients with 24 tumors, a significant correlation was found between the absorbed dose until best response and tumor response (Fig. 5). Consequently, responding PNETs have higher absorbed doses than nonresponding tumors. These higher absorbed doses emphasize the importance of delivering the highest possible activity to the tumor without exceeding the maximum acceptable doses to the critical organs. It is therefore of importance to



**FIGURE 4.** Example of dose response in patient with inoperable metastasized PNET in liver (patient 19). (A) Transversal contrast-enhanced CT images in late arterial phase. (B) Fused SPECT/CT images. Shown left to right are examinations at baseline and after 2 and 3 cycles of PRRT.

determine the definite maximum acceptable doses to the kidneys and bone marrow, which still are under discussion because these have been adopted from external-beam radiation therapy with different dose rates (12,15,17,26).

Although there was a clear correlation between the absorbed dose and tumor response, some lesions received a rather high absorbed dose but showed only minor reduction in size and vice versa. This wide range of absorbed doses is likely to be related to factors such as heterogeneity in binding affinity and receptor density, hypoxia, interstitial pressure, necrosis, and differences in tumor volume, and the wide range of tumor shrinkage is likely to be related to, for example, hypoxia, proliferation rate and necrosis. Altogether these factors potentially influence the tumor-specific radiosensitivity and the overall outcome of the therapy. Therefore, further studies are required in which these effects are evaluated in connection with PRRT.

Absorbed dose estimates during intermediate treatment cycles relied merely on the 24-h posttherapy images and on the assumption of unchanged effective half-life, compared with the previous complete dosimetric evaluation (19). As shown in the present results, it is a valid approximation to assume unchanged effective half-life, but for those patients for whom effective half-lives vary, the absorbed dose will be either overestimated or underestimated. Because complete dosimetric

evaluation at each therapy cycle is resource-demanding in terms of time on scanner and staff, and also somewhat uncomfortable for the patient, we have chosen to apply limited dosimetry during PRRT despite the inherent limitations with this approach, at the risk of yielding somewhat lower accuracy than with complete dosimetric evaluations.

In the absorbed dose calculations, we used the ACDF of a 10-g sphere instead of the ACDF of the actual tumor size, which might result in under- or overestimations of the calculated absorbed doses. However, for the range of tumor volumes in this study (4–25 mL), the ACDF varies from 0.0234 to 0.0237 mGy·g/MBq·s, compared with an ACDF of 0.0236 mGy·g/MBq·s for a 10-g sphere. This means that for 4-mL tumors, the overestimation of the absorbed doses is 0.7%, which we considered negligible in comparison with other uncertainties in the study.

The SPECT images used for activity concentration measurements are affected by limited spatial resolution, attenuation, and scatter, which degrade quantification and hence the absorbed dose calculations. Limited spatial resolution in SPECT leads to underestimation of the radioactivity concentration in tumors smaller than the spatial resolution. Consequently, to compensate for this effect we needed to apply RCs as determined from phantom measurements. However, for tumors smaller than 2.2 cm in diameter, accurate partial-volume correction is not possible because tumor size can no longer be accurately estimated from the SPECT images (Fig. 2). Therefore, these tumors were excluded from the study. Even in tumors larger than 2.2 cm, the PVE was still high and in order to further decrease the influence of PVE, the dose–response relationship was additionally determined for a subgroup of tumors with diameters larger than 4.0 cm. When Figures 5A and 5B are compared, it is evident that the degree of correlation increases with the tumor size because of the nearly full recovery obtained for the large tumors with less PVE. This improved correlation is at least partly due to the inherent errors in partial-volume correction. For example, for most tumors, the assumption of spherical lesions was probably true, but for some lesions mismatch of the volumes may have affected the quantitation of RC and thus the absorbed dose calculation. For nonspherical tumors, a small underestimation of the absorbed dose will occur. In addition, partial-volume correction as applied here assumes homogeneous tumor uptake, which is not necessarily true for all lesions but is difficult to assess in SPECT images because of their limited resolution.

One of the inclusion criteria in the study was the presence of a tumor with a diameter larger than 2.2 cm at any time during the treatment. This also means that responding tumors that shrunk to below 2.2 cm in diameter (according to diagnostic CT) during the course of the treatment were not included in the present work. Hence, the results of this study cannot be used to assess overall response to PRRT.

The SPECT images were corrected for limited spatial resolution and attenuation, but no correction was performed for scatter. Generally, scatter correction is achieved by applying a scatter energy window and subtracting the data obtained in this window from the ordinary energy window (27). Because the accuracy of this method is still a matter of discussion, we chose to refrain from using it in the present study. Also,

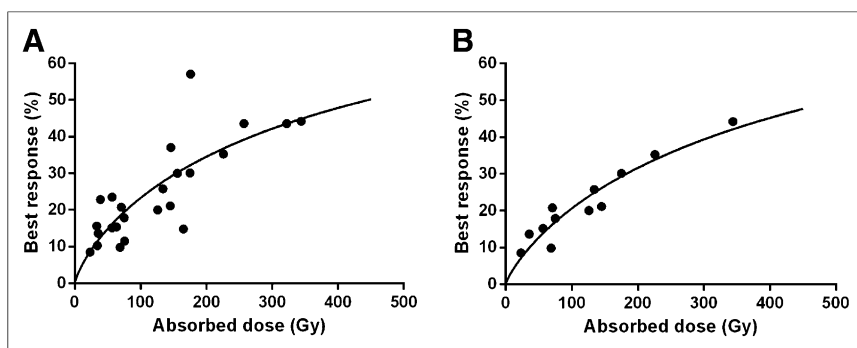


**FIGURE 5.** Tumor dose–response relationship for patients with PNETs treated with PRRT using  $^{177}\text{Lu}$ -DOTATATE, including tumors larger than 2.2 cm (A) and only tumors larger than 4 cm (B). Solid lines represent 2-parameter sigmoid fits ( $y = 100/(1 + (\alpha/x)^\beta)$ ), where  $\alpha$  and  $\beta$  are fitting parameters. Parameters  $\alpha$  and  $\beta$  were 445 and 0.79, with SEs of 104 and 0.14, respectively, for tumors larger than 2.2 cm and 504 and 0.84, with SEs of 83 and 0.1, respectively, for tumors larger than 4 cm. Pearson correlation coefficients ( $R^2$ ) were 0.64 (A) and 0.91 (B).

scatter correction mainly affects the radioactivity concentrations in low-activity areas and not as much in tumors with high uptake. In addition, because the scatter window can include events from the low-energy  $\gamma$  emitted by  $^{177}\text{Lu}$ , it is also from this aspect unknown whether this correction method can be applied for SPECT acquired during  $^{177}\text{Lu}$ -DOTATATE therapy. The contributions of downscatter from higher energy transitions (250 and 321 keV) into the applied energy window should be of little consequence because their abundance is less than 5% of that of the 208-keV  $\gamma$ .

Accurate quantification of the activity concentration in a tumor is not only determined by the imaging method but also greatly influenced by how the tumors are delineated. The most common method is based on a threshold setting for which the tumor is automatically delineated at a certain threshold, or cutoff level, of the maximum pixel value. In this study, a 42% threshold was applied because this generally corresponds best with the actual anatomic dimensions of the tumor at hybrid imaging (SPECT/CT, PET/CT). On examinations with low tumor-to-background contrast, this isocontour may be difficult to apply, such as in some  $^{18}\text{F}$ -FDG PET/CT examinations (28). However, in the present SPECT/CT examinations, the tumor-to-background ratios were generally high, and thus these possible drawbacks with the 42% threshold level were not likely to significantly decrease the precision of the measurements due to this level selection. As long as the size of the lesion is at least twice the spatial resolution, the threshold is relatively independent of source size and geometry (23). As evident in the subgroup analysis, by excluding tumors smaller than 4.0 cm in diameter the influence of PVE was decreased and variations in activity concentration by the choice of threshold setting were minimal. Thus, the accuracy of the absorbed dose calculations should improve.

## CONCLUSION

Calculations of tumor-absorbed doses during PRRT with  $^{177}\text{Lu}$ -DOTATATE are feasible. The findings of this study imply a clear correlation between the tumor-absorbed doses and tumor reduction in PNETs. The correlation coefficient was 0.64 for tumors larger than 2.2 cm in diameter and 0.91 for tumors larger than 4.0 cm. The outcome of the therapy effect in terms of tumor reduction is greater at higher absorbed doses. Although a significant correlation was found between the tumor-absorbed dose and tumor reduction, further studies are necessary to address the large variations in response for similar absorbed doses.

## DISCLOSURE

The costs of publication of this article were defrayed in part by the payment of page charges. Therefore, and solely to indicate this fact, this article is hereby marked "advertisement" in accordance with 18 USC section 1734. No potential conflict of interest relevant to this article was reported.

## ACKNOWLEDGMENT

We are grateful to the department of medical physics and the staff at the department of nuclear medicine and the endocrine oncology (78D) for their skilled assistance.

## REFERENCES

1. Kam BL, Teunissen JJ, Krenning EP, et al. Lutetium-labelled peptides for therapy of neuroendocrine tumours. *Eur J Nucl Med Mol Imaging*. 2012;39(suppl 1):S103–S112.

2. Kwekkeboom DJ, Teunissen JJ, Bakker WH, et al. Radiolabeled somatostatin analog [ $^{177}\text{Lu}$ -dota(0,tyr3)]octreotate in patients with endocrine gastroenteropancreatic tumors. *J Clin Oncol*. 2005;23:2754–2762.
3. Kwekkeboom DJ, de Herder WW, Kam BL, et al. Treatment with the radio-labeled somatostatin analog [ $^{177}\text{Lu}$ -DOTA(0,tyr3)]octreotate: toxicity, efficacy, and survival. *J Clin Oncol*. 2008;26:2124–2130.
4. Bergsma H, van Vliet EI, Teunissen JJ, et al. Peptide receptor radionuclide therapy (PRRT) for GEP-NETs. *Best Pract Res Clin Gastroenterol*. 2012;26:867–881.
5. Kwekkeboom DJ, Bakker WH, Kam BL, et al. Treatment of patients with gastroenteropancreatic (GEP) tumours with the novel radiolabelled somatostatin analogue [ $^{177}\text{Lu}$ -dota(0,tyr3)]octreotate. *Eur J Nucl Med Mol Imaging*. 2003;30:417–422.
6. Forrer F, Uusijarvi H, Storch D, Maecke HR, Mueller-Brand J. Treatment with  $^{177}\text{Lu}$ -DOTATOC of patients with relapse of neuroendocrine tumors after treatment with  $^{90}\text{Y}$ -DOTATOC. *J Nucl Med*. 2005;46:1310–1316.
7. Kwekkeboom DJ, Mueller-Brand J, Paganelli G, et al. Overview of results of peptide receptor radionuclide therapy with 3 radiolabeled somatostatin analogs. *J Nucl Med*. 2005;46(suppl 1):62S–66S.
8. Bodei L, Cremonesi M, Grana CM, et al. Peptide receptor radionuclide therapy with  $^{177}\text{Lu}$ -DOTATATE: the IEO phase I-II study. *Eur J Nucl Med Mol Imaging*. 2011;38:2125–2135.
9. Gabriel M, Andergassen U, Putzer D, et al. Individualized peptide-related radionuclide-therapy concept using different radiolabelled somatostatin analogs in advanced cancer patients. *Q J Nucl Med Mol Imaging*. 2010;54:92–99.
10. Yao JC, Hassan M, Phan A, et al. One hundred years after "carcinoid": epidemiology of and prognostic factors for neuroendocrine tumors in 35,825 cases in the united states. *J Clin Oncol*. 2008;26:3063–3072.
11. Garske-Roman U.  *$^{177}\text{Lu}$ -DOTA-Octreotate Radionuclide Therapy of Neuroendocrine Tumours: Dosimetry-Based Therapy Planning and Outcome* [PhD thesis]. Uppsala, Sweden: Uppsala University; 2012.
12. Sandström M, Garske-Roman U, Granberg D, et al. Individualized dosimetry of kidney and bone marrow in patients undergoing  $^{177}\text{Lu}$ -DOTA-octreotate treatment. *J Nucl Med*. 2013;54:33–41.
13. Sandström M, Garske U, Granberg D, Sundin A, Lundqvist H. Individualized dosimetry in patients undergoing therapy with  $^{177}\text{Lu}$ -DOTA-d-phe (1)-tyr (3)-octreotate. *Eur J Nucl Med Mol Imaging*. 2010;37:212–225.
14. Kwekkeboom DJ, Bakker WH, Kooij PP, et al. [ $^{177}\text{Lu}$ -dotaoty(3)]octreotate: comparison with [ $^{111}\text{In}$ -dtpao]octreotide in patients. *Eur J Nucl Med*. 2001;28:1319–1325.
15. Barone R, Borson-Chazot F, Valkema R, et al. Patient-specific dosimetry in predicting renal toxicity with  $^{90}\text{Y}$ -DOTATOC: relevance of kidney volume and dose rate in finding a dose-effect relationship. *J Nucl Med*. 2005;46(suppl 1):99S–106S.
16. Emami B, Lyman J, Brown A, et al. Tolerance of normal tissue to therapeutic irradiation. *Int J Radiat Oncol Biol Phys*. 1991;21:109–122.
17. Cremonesi M, Ferrari M, Bodei L, Tosi G, Paganelli G. Dosimetry in peptide radionuclide receptor therapy: a review. *J Nucl Med*. 2006;47:1467–1475.
18. Pauwels S, Barone R, Walrand S, et al. Practical dosimetry of peptide receptor radionuclide therapy with  $^{90}\text{Y}$ -labeled somatostatin analogs. *J Nucl Med*. 2005;46(suppl 1):92S–98S.
19. Garske U, Sandstrom M, Johansson S, et al. Minor changes in effective half-life during fractionated  $^{177}\text{Lu}$ -octreotate therapy. *Acta Oncol*. 2012;51:86–96.
20. Forrer F, Krenning EP, Kooij PP, et al. Bone marrow dosimetry in peptide receptor radionuclide therapy with [ $^{177}\text{Lu}$ -DOTA(0,tyr3)]octreotate. *Eur J Nucl Med Mol Imaging*. 2009;36:1138–1146.
21. Srinivas SM, Dhurairaj T, Basu S, Bural G, Surti S, Alavi A. A recovery coefficient method for partial volume correction of pet images. *Ann Nucl Med*. 2009;23:341–348.
22. National Electrical Manufacturers Association (NEMA). *Performance Measurements of Positron Emission Tomographs*. NEMA Standards Publication NU 2-2001: Washington, D.C.: National Electrical Manufacturers Association; 2001.
23. Erdi YE, Wessels BW, Loew MH, Erdi AK. Threshold estimation in single photon emission computed tomography and planar imaging for clinical radioimmunotherapy. *Cancer Res*. 1995;55:5823s–5826s.
24. Jentzen W, Weise R, Kupferschlager J, et al. Iodine-124 PET dosimetry in differentiated thyroid cancer: recovery coefficient in 2d and 3d modes for PET(CT) systems. *Eur J Nucl Med Mol Imaging*. 2008;35:611–623.
25. Eisenhauer EA, Therasse P, Bogaerts J, et al. New response evaluation criteria in solid tumours: revised RECIST guideline (version 1.1). *Eur J Cancer*. 2009;45:228–247.
26. Bodei L, Cremonesi M, Ferrari M, et al. Long-term evaluation of renal toxicity after peptide receptor radionuclide therapy with  $^{90}\text{Y}$ -dotatoc and  $^{177}\text{Lu}$ -DOTATATE: the role of associated risk factors. *Eur J Nucl Med Mol Imaging*. 2008;35:1847–1856.
27. Koral KF, Swailen FM, Buchbinder S, Clinthorne NH, Rogers WL, Tsui BM. SPECT dual-energy-window Compton correction: scatter multiplier required for quantification. *J Nucl Med*. 1990;31:90–98.
28. Boellaard R, O'Doherty MJ, Weber WA, et al. FDG PET and PET/CT: EANM procedure guidelines for tumour PET imaging: version 1.0. *Eur J Nucl Med Mol Imaging*. 2010;37:181–200.